Published in final edited form as:
Acta Biomater. 2014 October ; 10(10): 4484–4493. doi:10.1016/j.actbio.2014.06.027.

Human embryonic stem cells and macroporous calcium phosphate construct for bone regeneration in cranial defects in rats

Xian Liu[1,2,#], **Ping Wang**[1,2,#], **Wenchuan Chen**[1,2], **Michael D. Weir**[1], **Chunyun Bao**[2], and **Hockin H. K. Xu**[1,3,4,5,*]

[1]Biomaterials & Tissue Engineering Division, Department of Endodontics, Prosthodontics and Operative Dentistry, University of Maryland Dental School, Baltimore, MD 21201, USA

[2]State Key Laboratory of Oral Diseases, West China Hospital of Stomatology, Sichuan University, Chengdu, Sichuan 610041, China

[3]Mechanical Engineering Department, University of Maryland Baltimore County, Baltimore, MD 21250, USA

[4]Center for Stem Cell Biology and Regenerative Medicine, University of Maryland School of Medicine, Baltimore, MD 21201, USA

[5]University of Maryland Marlene and Stewart Greenebaum Cancer Center, University of Maryland School of Medicine, Baltimore, MD 21201, USA

Abstract

Human embryonic stem cells (hESCs) are an exciting cell source to offer an unlimited supply of cells that can differentiate into all cell types for regenerative medicine applications. To date, there has been no report on hESCs with calcium phosphate cement (CPC) scaffolds for bone regeneration in vivo. The objectives of this study were to: (1) investigate hESCs for bone regeneration in vivo in critical-sized cranial defects in rats; (2) determine the effects of cell seeding and platelets in macroporous CPC on new bone and blood vessel formation. hESCs were cultured to yield mesenchymal stem cells (MSCs), which underwent osteogenic differentiation. Four groups were tested in rats: (1) CPC control without cells; (2) CPC with hESC-derived MSCs ("CPC+hESC-MSC"); (3) CPC with hESC-MSCs and 30% human platelet concentrate (hPC) ("CPC+hESC-MSC+30%hPC"); (4) CPC+hESC-MSC+50%hPC. In vitro, MSCs were derived from embryoid bodies (EBs) of hESCs. Cells on CPC were differentiated into the osteogenic lineage, with highly-elevated alkaline phosphatase (ALP) and osteocalcin (OC) expressions as

Correspondence: Dr. Hockin H. K. Xu, Professor, Director of Biomaterials & Tissue Engineering Division, Department of Endodontics, Prosthodontics and Operative Dentistry, University of Maryland Dental School, Baltimore, MD 21201 (hxu@umaryland.edu). Dr. Chongyun Bao, Professor, West China College of Stomatology, Sichuan University, China (cybao9933@yahoo.com.cn).
[#]These two authors contributed equally.

well as mineralization. In vivo at 12 weeks, groups with hESC-MSCs and hPC had new bone 3-times, and blood vessel density 2-times, those of CPC control. The new bone in the defects contained osteocytes and blood vessels, and the new bone front was lined with osteoblasts. The group with 30% hPC and hESC-MSCs had a blood vessel density that was 49% greater than the hESC-MSC group without hPC, likely due to the various growth factors in the platelets enhancing both new bone and blood vessel formation. In conclusion, hESCs are promising for bone tissue engineering, and hPC can enhance new bone and blood vessel formation. Macroporous CPC with hESC-MSCs and hPC may be useful for bone regeneration in craniofacial and orthopedic applications.

Keywords

Calcium phosphate cement; Human embryonic stem cells; Human platelet concentration; Bone regeneration; Athymic rats; Critical-sized cranial defect

1. Introduction

Reconstruction of massive bone defects is a challenging problem to orthopedic surgeons in clinic. Although autografts are regarded as the gold-standard for filling bone defects, their applications are greatly restricted by harvest limitation, donor-site morbidity and other complications. Therefore, there is an urgent need for developing new bone substitutes to avoid or minimize the demand for autologous bone grafts, especially in bridging massive bone defects. Bone tissue engineering and regenerative medicine emerge as a promising option [1–3]. A combination of three-dimensional scaffolds, stem cells, and growth factors could orchestrate the bone regeneration process in a synergistic way [4–6]. Substantial efforts have been made in this field yielding promising results [7–9]. A biocompatible scaffold that mimics natural bone extracellular matrix plays a key role for successful regeneration [10–12]. Due to their chemical and crystallographic similarities to the inorganic components of bone matrix, calcium phosphate (CaP) biomaterials are useful for bone repairs [13–20]. Among them, calcium phosphate cements are biocompatible and osteoconductive, and can be resorbed and replaced by new bone [21–25]. The first calcium phosphate cement (referred to as CPC) was comprised of tetracalcium phosphate (TTCP) and dicalcium phosphate-anhydrous (DCPA) [21,26]. The CPC powder can be mixed with an aqueous liquid to form a paste that can be sculpted during surgery to conform to the defects, and the paste self-hardens to form resorbable hydroxyapatite [21,26]. Since then, several other novel compositions of calcium phosphate cements were developed with bone regeneration applications [22–25,28]. Recent studies on CPC focused on improving bone formation by creating macropores, seeding stem cells and delivering growth factors [27–31].

Human embryonic stem cells (hESCs) are an exciting stem cell source that offer a high potential for tissue regeneration due to the primitive nature of the cells [13,32–36]. In addition, hESCs offer the ability for rapid proliferation to provide an unlimited supply of stem cells for regenerative medicine applications. hESCs can differentiate into all bone formation-related cells, such as mesenchymal cells [32–35], osteoblasts [36,37], endothelial cells [38], and neurons [39]. hESCs with osteogenic differentiation can form human bone after being implanted in bone defects or transplanted subcutaneously [33,36]. Several other

reports also demonstrated bone formation via hESCs [13,40–44]. Recently, hESC-derived mesenchymal stem cells (referred to as hESC-MSCs) were seeded on CPC scaffolds and showed promising results in vitro [31,45]. However, there has been no report on the use of hESCs with CPC for in vivo bone regeneration.

Besides scaffolds and stem cells, growth factors are also important for tissue engineering. Platelet-rich plasma (PRP) is an autologous blood-derived product, with platelet-derived growth factors to aid osteogenesis and bone formation [46,47]. In a study on rat bone marrow stromal cell differentiation, the addition of platelets enhanced the expression of vascular endothelial growth factor (VEGF) and platelet-derived growth factor (PDGF) [48]. VEGF and PDGF are important for recruiting endothelial cells in vivo to start the angiogenesis process [48]. Platelets could also help recruit MSCs to the altered vascular wall and enhance biological functions of MSCs [49]. Thus, platelets may represent an important bridging mechanism of recruiting endothelial cells and MSCs. However, the benefit of PRP has not been consistently reported; for example, two reports found no significant difference in bone formation using BMSC-seeded calcium-deficient hydroxyapatite scaffold with or without PRP [50,51]. In addition, the use of platelets with hESCs and CPC has not been investigated.

Therefore, the objectives of this study were to: (1) investigate hESCs for bone regeneration in vivo in critical-sized cranial defects in rats; (2) determine the effects of cell seeding and platelets in macroporous CPC scaffold on new bone and blood vessel formation. The following hypotheses were tested: (1) hESC-MSCs seeded in CPC scaffold would generate much more bone and blood vessels than CPC control without cell seeding; (2) the addition of platelets in hESC-MSC-seeded CPC construct would generate more new bone and higher blood vessel density than hESC-MSC-seeded CPC without platelets.

2. Materials and methods

2.1. hESC culture and MSC derivation

The use of hESCs (H9, Wicell, Madison, WI) was approved by the University of Maryland Institutional Review Board and followed the Wicell protocol. hESCs were cultured to form three-dimensional cell aggregates called embryoid bodies (EBs), and MSCs were then migrated out of the EBs [13,31,33,41,45]. First, undifferentiated hESCs at passage 36 were cultured as colonies on a feeder layer of mitotically inactivated murine embryonic fibroblasts (MEF). Aggregates of undifferentiated hESCs were dissociated into clumps of approximately 0.5 mm in diameter and cultured on 25 cm^2 ultra-low attachment culture flasks (Corning, Corning, NY) to form hESC-EBs. The EB medium consisted of high glucose Dulbecco's modified Eagle medium (DMEM) (Invitrogen, Carlsbad, CA) supplemented with 20% embryonic stem cell-qualified fetal bovine serum (FBS) (catalog number 16141, Invitrogen) which was specially tested for the ability to sustain undifferentiated cellular morphology of embryonic stem cells, 1 mM glutamine (Sigma, St. Louis, MO), 0.1 mM 2-mercaptoethanol (Sigma) and 1% MEM non-essential amino acids solution (Invitrogen). Then, hESC-EBs were transferred into six-well plates (Nunclon Δ Surface, Nunc, Rochester, NY) for further culture, and cells were sprouted and migrated out of the EBs spontaneously. These outgrowth cells were isolated by using cell scrapers and

cultured in MSC growth medium, which consisted of DMEM (Gibco, Gaithersburg, MD) supplemented with 10% FBS (HyClone, Logan, UT), 2 mM L-glutamine (Gibco), 100 U/mL penicillin, and 100 mg/mL streptomycin (Gibco) of DMEM (Gibco). These cells were characterized in our previous studies via flow cytometry, and the MSC surface markers were consistently and highly expressed [31,45]. The MSC surface markers CD29, CD44, CD73, and CD166 were expressed to levels > 99.4%. On the other hand, the expressions of hematopoietic markers (CD31, CD34, CD45) were less than 1.5%. Furthermore, HLA-ABC was expressed at 94.1%, whereas HLA-DR, TRA-1-81 and Oct3/4 were absent, which is characteristic for MSCs [31,45]. The derivation of MSCs from hESCs was consistent with previous studies [13,41].

2.2. Development of macroporous CPC scaffold

The CPC powder consisted of an equimolar mixture of TTCP ($Ca_4[PO_4]_2O$) and DCPA ($CaHPO_4$) [26]. TTCP was synthesized using DCPA and calcium carbonate (both from J.T. Baker, Philipsburg, NJ) which were mixed and heated at 1500 °C for 6 h in a furnace (Model 51333, Lindberg, Watertown, WI). The heated mixture was quenched to room temperature in a desicator, ground in a ball mill (Retsch PM4, Brinkman, NY) and sieved to obtain TTCP powder with a median particle size of 17 μm. The commercial DCPA powder was ground for 24 h in the ball mill in 95 % ethanol and sieved to obtain a median particle size of approximately 1 μm. Then the TTCP and DCPA powders at 1:1 molar ratio were thoroughly mixed in a micromill (Bel-Alert Products, Pequannock, NJ) to form the CPC powder [21,26,52]. Rod-shaped, water-soluble mannitol crystals were used as porogen to produce macropores in CPC [27,52]. Mannitol particles ($CH_2OH[CHOH]_4CH_2OH$, Sigma) with sizes of 125 μm to 250 μm were mixed with CPC powder at a mannitol powder/(CPC powder + mannitol powder) = 40% by mass, following previous studies [27,52]. A 0.25 mol/L sodium phosphate solution (Na_2HPO_4) solution was used as the CPC liquid for fast-setting [52]. The powder/liquid mass ratio was 2:1, and the mixed paste was placed into a mold with a diameter of 8 mm and a thickness of 1 mm [53]. The specimen was incubated in a humidor at 37 °C for 4 h, then demolded and immersed in water at 37 °C for 20 h. In this process, mannitol particles were dissolved and macropores were created in CPC [52]. To measure the porosity, CPC specimens were dried in a vacuum oven (Model DP-21, American Scientific Products, McGaw Park, IL) at 60 °C for 24 h. The density was measured using specimen weight divided by specimen volume, following a previous study [52]. The volume was calculated by the specimen dimensions measured with a micrometer, with each dimension the average of three locations for each specimen. The porosity was estimated as: $P = (d_{HA} - d_{CPC})/d_{HA}$, where d_{HA} is the density of fully-dense hydroxyapatite (3.14 g/cm^3) [52], and d_{CPC} is the measured CPC density.

2.3. hESC-MSC seeding on macroporous CPC scaffold

CPC scaffolds were sterilized in an ethylene oxide sterilizer (Andersen, Haw River, NC) for 12 h and incubated with culture medium for 3 h prior to cell seeding. Passage 3 hESC-MSCs were used for the experiments of this study. A density of 1.5×10^5 cells were seeded into each well containing a CPC scaffold disk with 2 mL osteogenic medium in a 24-well plate. The osteogenic medium consisted of the growth medium plus 100 nM dexamethasone, 10

mM β-glycerophosphate, 0.05 mM ascorbic acid, and 10 nM 1α,25-Dihydroxyvitamin (Sigma) [3,31,45].

After culturing in the osteogenic medium for 1, 4, 7 or 14 d, the hESC-MSCs on CPC scaffold were stained using a live/dead viability kit (Molecular Probes, Eugene, OR) and viewed via epifluorescence microscopy (TE2000-S, Nikon, Melville, NY). The percentage of live cells was measured as: L = number of live cells/(number of live cells + number of dead cells). The live cell density was measured as: D = number of live cells in the image/the image area [27,53]. Three randomly-chosen fields of view were photographed for each specimen. Five specimens of each group (n = 5) yielded 15 images for each time point. In addition, scanning electron microscopy (SEM, Quanta 200, FEI, Hillsboro, OR) was used to examine the CPC scaffold without cells and with cell seeding after 7 d of culture.

2.4. Osteogenic gene expressions of hESC-MSCs on CPC

Quantitative real-time reverse transcription polymerase chain reaction (qRT-PCR, 7900HT, Applied Biosystems, Foster City, CA) method was used to measure the osteogenic differentiation of hESC-MSCs on CPC scaffold. After 1, 4, 7 and 14 d of culturing in osteogenic medium, the total cellular RNA on the scaffold was extracted with TRIzol reagent (Invitrogen), and reverse-transcribed into cDNA using a High-Capacity cDNA Reverse Transcription kit (Applied Biosystems) in a thermal-cycler (GenAmp PCR 2720, Applied Biosystems). TaqMan gene expression assay kits, including two pre-designed specific primers and probes, were used to measure the transcript levels of the proposed genes on human alkaline phosphatase (ALP, Hs00758162_ml, RefSeq NM_000478.4, assay location: 1120, amplicon length: 84; RefSeq NM_001127501.2, assay location: 955, amplicon length: 84; RefSeq NM_001177520.1, assay location: 839, amplicon length: 84), osteocalcin (OC, Hs00609452_g1, RefSeq NM_199173.4, assay location: 178, amplicon length: 74), Runt-related transcription factor 2 (Runx2, Hs00231692_ml, RefSeq NM_001015051.3, assay location: 900, amplicon length: 116; RefSeq NM_001024630.3, assay location: 900, amplicon length: 116; RefSeq NM_001278478.1, assay location: 648, amplicon length: 116), and glyceraldehyde 3-phosphate dehydrogenase (GAPDH, Hs99999905, RefSeq NM_002046.4, assay location: 229, amplicon length: 122) [29,31]. Relative expression level for each target gene was evaluated using the $2\text{-}\Delta\Delta C_t$ method [54]. The C_t of hESC-MSCs cultured on CPC for 1 d served as the calibrator. The C_t values of target genes were normalized by the C_t values of the human housekeeping gene GAPDH to obtain the ΔC_t values [29,31,55].

2.5. Mineral synthesis by hESC-MSCs on CPC in vitro

After 1, 4, 7 and 14 d, hESC-MSCs on CPC were fixed with 10% formaldehyde and stained with Alizarin Red S (ARS, Millipore, Billerica, MA). The ARS stained calcium-rich deposits by cells into a red color. An osteogenesis assay (Millipore) was used to extract the stained minerals and measure the ARS concentration at OD_{405}, following the manufacturer's instructions [53]. The ARS standard curve was constructed with known concentration of the dye [53]. CPC disks without cells served as control, and were immersed and measured in the same manner. The control's ARS concentration was subtracted from the ARS concentration

of disks with cells to yield the net mineral concentration synthesized by cells, following previous studies [53].

2.6. In vivo animal experiment and surgical procedures

hESC-MSCs were seeded on CPC scaffold disks and cultured in osteogenic medium for 14 d as described above. Then the cell-seeded scaffolds were taken out of the medium, and incubated in 500 μL osteogenic medium with the addition of human platelet concentrate (hPC, at 1.2×10^6 platelets per μL, Biological Specialty, Colmar, PA) for 1 hour. The hPC was activated using 25 μL of 10% calcium chloride, which formed a soft gel film binding to and covering the scaffold disk. This scaffold construct was then implanted *in vivo*. Three hPC concentrations were tested: 0% (osteogenic medium with no hPC), 30% hPC in osteogenic medium (0.36×10^6 platelets/μL), and 50% hPC in medium (0.6×10^6 platelets/μL). Four groups were tested in rats:

- **i.** CPC scaffold control disks without cells;
- **ii.** CPC seeded with hESC-MSCs (referred to as “CPC+hESC-MSC” group);
- **iii.** CPC seeded with hESC-MSCs and 30% hPC (“CPC+hESC-MSC+30%hPC”);
- **iv.** CPC seeded with hESC-MSCs and 50% hPC (“CPC+hESC-MSC+50%hPC”).

Twenty-four athymic nude rats (200–250 g, Harlan, Indianapolis, IN) were used, with six rats for each group (n = 6). The critical-sized cranial defect model in rats [2,9] was approved by the University of Maryland Baltimore (IACUC # 0909014) [53]. All procedures involving animals followed NIH animal care guidelines. The rats were anesthetized by intraperitoneal injection of a combination of 75 mg/kg body-weight of ketamine and 10 mg/kg of xylazine [53]. An approximately 2 cm mid-longitudinal incision was made on the dorsal surface of the cranium. The periosteum of cranium was completely cleared off. An 8-mm circular bone defect was created with a trephine bur, and the full thickness of cranial bone was removed under constant irrigation with sterile saline [2]. A CPC disk was placed in the defect and the incision was closed using 4-0 resorbable sutures. For the cell-seeded groups, the cell-seeded surface of the scaffold was implanted in contact with the dura of the rats [53]. After 12 weeks of implantation, the rats were sacrificed with carbon monoxide. Specimens were fixed in 10% zinc-buffered formalin and then analyzed [53].

2.7. Histomorphometric analysis

Specimens were processed for decalcification in 30% buffered formic acid for 7 d at room temperature [53]. After dehydration and clearing, the specimens were embedded in paraffin and the central part of the implant and defect was cut into 5 μm thick sections. The sections were stained with hematoxylin and eosin (H&E). Image Pro Plus Software (Media Cybernetics, Carlsbad, CA) was used to examine the histological images. The perimeter around the new bone was traced, and the area of the new bone was measured by the software. New bone area fraction was calculated as the new bone area in the defect divided by the entire defect area. Blood vessels were identified by their luminal structure and the presence of red blood cells within their boundaries. The new vessel density was determined by the number of blood vessels in the defect area divided by the entire defect area [53]. One

section from the central part of the implant for each rat was analyzed and the average value of each group (n = 6) was obtained for each group.

2.8. Statistical analysis

Statistical analyses were performed using Statistical Package for the Social Sciences (SPSS 16.0, Chicago, IL). Levene test was first performed to confirm that the normality and equal variance assumptions of the data were not violated. Statistical significance was assessed by using one-way analysis of variance (ANOVA) followed by post-hoc LSD (least significant difference) tests. A confidence level of 95% ($p < 0.05$) was considered to be statistically significant.

3. Results

Fig. 1(A–D) show representative SEM images of CPC scaffold before cell seeding. Examination of the specimens indicated that the pores from mannitol dissolution had sizes ranging from about 100 μm to 300 μm. Smaller pores of about 1 μm to 50 μm were also present. The pores appeared to be well-formed in the shapes of the entrapped mannitol crystals. Arrows in Fig. 1(A–D) indicate fenestrations in the pore walls and bottoms leading to the next pores, indicating pore interconnection. Fig. 1E shows a typical image of hESC-MSCs seeded on CPC scaffold at an intermediate 7 d. The cells appeared to be well attached to CPC surface, with a spreading morphology and long cytoplasmic extensions. Arrows in (E) indicate the approximate boundary of a macropore in CPC, which received infiltration of numerous cells.

Fig. 2A–D shows representative live/dead images of hESC-MSCs on CPC scaffolds cultured in osteogenic medium for 1, 4, 7 and 14 d, respectively. The live cell density increased with time on CPC due to proliferation. The percentages of live cells were approximately 80–90% (E). The live cell density (F) increased more than 6-fold from 1 to 14 d. These results indicate that hESC-MSCs exhibited good viability and compatibility with CPC scaffold.

The osteogenic differentiation and mineral synthesis results in vitro are plotted in Fig. 3. The RT-PCR results on gene expressions of ALP, OC and Runx2 are shown in (A–C). The osteogenic gene expressions increased with time, and the 14 d values were 6 to 25 folds of those at 1 d ($p < 0.001$). Results on hESC-MSC-synthesized minerals measured by the osteogenesis assay are plotted in (D). The mineral synthesis by hESC-MSCs increased by 5-fold from 4 to 14 d ($p < 0.001$). The minerals synthesized by the hESC-MSCs were stained red by ARS staining, with examples shown in (E). The ARS staining of the cell-synthesized bone matrix materials became thicker and darker form 4 to 14 d, indicating that the mineral synthesis increased with time, consistent with the results in (D).

During the implantation of 12 weeks, all animals survived. They appeared normal and healthy, with no evidence of infection. Representative H&E images are shown in Fig. 4. Mineralized new bone was observed in all groups. Examination of all samples indicated that there was more new bone in the groups with hESC-MSCs than CPC control without cells. There was more new bone when hPC was used compared to that without hPC. Arrows indicate new bone. In each sample, while there was more new bone around the peripheral

sides of CPC scaffold, there was also new bone inside the CPC, indicating new bone ingrowth into the scaffolds. An example in (D) shows that the new bone not only extended across the entire dura side of the scaffold, but also grew into the interior of the CPC scaffold throughout the entire defect.

New bone formation in the defects could be seen by the appearance of osteoid with osteocytes and blood vessels, and with the newly-formed bone being lined by osteoblasts. The presence of osteocytes indicated the maturing of the new bone. Typical examples of these features are shown in Fig. 5A. The calcified new bone area had a more dark-red staining and a densely-organized matrix. The uncalcified new bone matrix had a light red staining and a loosely-structured matrix, which could become calcified over time in vivo. Examples of these areas are shown in (B).

Quantitative histomorphometric results are plotted in Fig. 6. Seeding hESC-MSCs to CPC scaffold generated more new bone than CPC control ($p = 0.002$). Adding 30% hPC to the CPC-hESC-MSC construct further increased new bone generation ($p = 0.021$). However, adding 50% hPC yielded results similar to those of 30% hPC ($p = 0.075$). The groups with hESC-MSCs and hPC had calcified new bone 3-fold, and blood vessel density around 2-fold those of CPC control.

4. Discussion

The present study investigated hESC-MSCs seeded on CPC scaffold for bone regeneration in rats in vivo for the first time. The results showed that hESC-MSCs attached well to CPC and had good proliferation and osteogenic differentiation. Groups with hESC-MSC seeding had much more new bone formation and blood vessel density in vivo than CPC control without cells. Adding hPC further significantly increased bone regeneration and blood vessel density than that without hPC. These results indicate that hESCs are promising for bone tissue engineering applications, and macroporous CPC scaffolds can be used to deliver hESC-MSCs with hPC to enhance bone regeneration.

ALP is a well-defined marker for osteogenic differentiation and expressed in the early stage of MSC osteogenesis, and its upregulation is considered a prerequisite for mineralization and subsequent maturing of bone [55]. OC and Runx2 also played key roles in the osteogenic differentiation of hESC-MSCs in previous studies [13,41]. In the present study, ALP, OC and Runx2 gene expressions were all highly upregulated for hESC-MSCs on CPC scaffold, suggesting that the hESC-MSCs successfully differentiated into the osteogenic lineage. This was corroborated with ARS staining and mineral synthesis by the cells in vitro. These results were consistent with previous studies on hESC-MSC seeding on CPC materials [31,45], and demonstrated that CPC could be a promising scaffold for hESC-MSC-based bone tissue engineering. However, the previous CPC scaffolds with hESC-MSCs were tested in vitro, with no in vivo results.

Several studies were performed to investigate hESCs for in vivo bone engineering [13,37,40–44]. However, there has been no report on hESC seeding with CPC for in vivo bone regeneration. In the present study, the hESC-MSC group generated new bone that was 2-fold that of CPC control, demonstrating the contribution of hESC-MSCs to bone

formation. The group with hESC-MSCs and 50% hPC generated new bone that was 3-fold that of CPC control. It is interesting to compare the enhancement of new bone via hESC-MSCs with human bone marrow mesenchymal stem cells (hBMSC). A previous study indicated that hBMSCs seeded on tripeptide arginyl-glycyl-aspartic acid (RGD)-grafted CPC scaffold achieved a new bone fraction of 24.9% at 12 weeks with the same cranial defect model in rats [53]. This value is consistent with the new bone amount generated by hESC-MSCs in the present study.

Platelet-rich plasma (PRP) is an autologous and easily isolated blood-derived product. PRP has benefits to be used with biomaterials for bone tissue engineering, because PRP could enhance tissue healing at the cellular level via the recruitment, proliferation and differentiation of cells [47–49,56]. There were reports on the combination of scaffold, stem cells and PRP for in vivo bone tissue engineering, for example, in comparing scaffold alone with scaffold plus stem cells plus PRP [57,58]. Two reports compared BMSC-seeded scaffold with BMSC-seeded scaffold plus PRP, and there was no enhancement in tissue regeneration via PRP in this system [50,51]. However, another report indicated that PRP combined with scaffold and BMSCs generated more new bone than BMSCs with scaffold without PRP [59]. Therefore, the effect of PRP on bone regeneration had contradictory results in previous studies; hence the PRP effect requires further study. Furthermore, there has been no report on the use of PRP with hESC-MSCs in CPC scaffold.

In addition, different PRP concentrations used for bone formation also showed conflicting results [60–62]. If the PRP concentrations were too high or too low, then the use of PRP was not beneficial, or even disadvantageous, for cell-based bone regeneration [63,64]. A study reported that the cells had the highest proliferation when using 30% platelet concentration (with a platelet concentration of 0.33×10^6 platelets per μL), while higher concentrations yielded less cell growth and decreased cell viability and proliferation [63]. This may be because the presence of substantial amounts of plasma in the platelet concentrate suppressed the cellular viability and proliferation, since plasma was shown to decrease the viability and proliferation of cells [63]. In the present study, CPC-hESC-MSCs were combined with hPC to enhance bone regeneration. Two hPC concentrations of 30% (0.36×10^6/μL) and 50% (0.6×10^6/μL) were tested based on previous studies. The results showed that both 30% and 50% hPC with CPC-hESC-MSCs had more new bone than CPC+hESC-MSC without hPC. Therefore, hPC was beneficial for hESC-MSCs in CPC for bone regeneration. However, there was no difference between 30% and 50% hPC. Two reasons likely contributed to this: (1) both 30% hPC and 50% hPC can increase cell viability and proliferation, but such increase may have been plateaued after 30% hPC; (2) while a higher hPC concentration may provide more growth factors to enhance cell differentiation and tissue formation, a higher hPC concentration may reduce cell growth and proliferation due to an increased amount of plasma [63].

Platelets contain a variety of growth factors, including transforming growth factors, platelet-derived growth factor (PDGF), insulin-like growth factor (IGF), epidermal growth factor (EGF), and epithelial cell growth factor (ECGF). These growth factors were reported to help induce bone formation or promote bone regeneration [65,66]. Angiopoietin-2 (Ang-2), platelet-derived endothelial cell growth factor (PDECGF), thrombospondin-1 and vascular

endothelial growth factor (VEGF) were all shown to be involved in bone regeneration [65,66]. In addition, these platelet factors were also critically important for angiogenesis. Angiogenesis helps deliver oxygen and nutrients to the cells and ensure the survival and function of the implanted and recruited cells, thus plays a key role in bone tissue engineering [12]. In the present study, the group with 30% hPC had a blood vessel density of 30.9 vessels/mm^2, while the hESC-MSC group without hPC had 20.8 vessels/mm^2. Therefore, the hPC delivery enhanced angiogenesis by 49% compared to the hESC-MSC group without hPC. This result was consistent with a previous report showing a 33.3% increase in vessel number compared to BMSC-seeded scaffold group without platelets [51]. In addition, the present study showed that the CPC+hESC-MSC group (no hPC) generated more blood vessels than the CPC control group without cells. This enhancement may be a contribution of the seeded hESC-MSCs, as CPC+hESC-MSCs clearly had more new bone and blood vessels than CPC control. Furthermore, previous studies showed that angiogenesis was positively correlated with bone formation rate [67,68]. This is consistent with the present study, which showed that the groups that generated a higher blood vessel density also had greater new bone formation. Another point that should be noted is that the periosteum was removed in this animal model, which is a more vigorous and strict test for the scaffold construct to regenerate new bone without the help from the periosteum. The removal of the periosteum followed previous investigators' protocols in animal studies [69–71].

The use of hESCs or their derivatives has several advantages over adult stem cells. First, hESCs possess robust proliferation and indefinite self-renewal ability to produce unlimited amounts of stem cells for tissue regeneration, compared to the limited proliferation of adult stem cells, especially for adult stem cells of patients with diseases or disorders. Second, the ability of hESCs to differentiate into all types of cells for the three germ layers is far superior to the lineage-specific differentiation of adult stem cells [72]. Therefore, the derivation of osteogenic cells from hESCs represents a potent alternative to adult stem cells for bone regeneration. However, the application of hESCs is restricted by ethical concerns, risks of teratoma formation and possible immune rejection. Patient-specific human induced pluripotent stem cells (hiPSCs) with similar proliferation and differentiation ability as hESCs have the potential to overcome some of these hurdles. Therefore, even if the therapeutic application of hESCs in the clinical arena has hurdles, the research findings on hESCs have transferable value to hiPSCs [73]. This is the first study investigating the repair of critical-sized bone defects by hESC-MSC-CPC constructs. It demonstrated the promise of hESC-MSC-CPC constructs for bone regeneration and the benefit of co-delivering hPC. However, bone regeneration efficiency can be further increased through efforts to accelerate resorption of the scaffold and to manipulate stem cell-microenvironment interactions. Further study is needed to investigate in these directions and also to test if the beneficial bone regeneration and blood vessel formation in rats can be similarly achieved in larger defects using a larger animal model.

5. Conclusions

The present study showed the promise of using hESCs for bone regeneration in vivo. hESC-MSCs were seeded on macropores CPC scaffolds with hPC delivery, and the constructs successfully generated new bone and blood vessels in cranial defects in rats. The groups

with hESC-MSCs and hPC had calcified new bone amount 3-times, and blood vessel density 2-times, those of CPC control. The new bone formed in the defect contained osteocytes and blood vessels, and the new bone front was lined with osteoblasts. The group with 30% hPC had a blood vessel density that was 49% greater than the counterpart without hPC, likely due to the various growth factors in the platelets enhancing both new bone and blood vessel formation. These results support the use of hESCs for regenerative medicine applications, and demonstrate the promise of hESC-MSC seeded CPC constructs with hPC co-delivery for bone tissue engineering.

Acknowledgments

We thank Dr. Carl G. Simon, Dr. Lawrence C. Chow, and Dr. David J. Mooney for discussions. This study was supported by NIH R01 DE14190 and R21 DE22625 (HX), Maryland Stem Cell Research Fund (HX), and University of Maryland School of Dentistry.

References

1. Steinert AF, Rackwitz L, Gilbert F, Noth U, Tuan RS. Concise review: the clinical application of mesenchymal stem cells for musculoskeletal regeneration: current status and perspectives. Stem Cells Transl Med. 2012; 1:237–47. [PubMed: 23197783]
2. O'Keefe RJ, Mao J. Bone tissue engineering and regeneration: from discovery to the clinic--an overview. Tissue Eng Part B Rev. 2011; 17:389–92. [PubMed: 21902614]
3. Salinas CN, Anseth KS. Mesenchymal stem cells for craniofacial tissue regeneration: designing hydrogel delivery vehicles. J Dent Res. 2009; 88:681–92. [PubMed: 19734453]
4. Gandavarapu NR, Mariner PD, Schwartz MP, Anseth KS. Extracellular matrix protein adsorption to phosphate-functionalized gels from serum promotes osteogenic differentiation of human mesenchymal stem cells. Acta biomater. 2013; 9:4525–34. [PubMed: 22982322]
5. Lim CT, Ren X, Afizah MH, Tarigan-Panjaitan S, Yang Z, Wu Y, et al. Repair of osteochondral defects with rehydrated freeze-dried oligo [poly(ethylene glycol) fumarate] hydrogels seeded with bone marrow mesenchymal stem cells in a porcine model. Tissue Eng Part A. 2013; 19:1852–61. [PubMed: 23517496]
6. Kretlow JD, Spicer PP, Jansen JA, Vacanti CA, Kasper FK, Mikos AG. Uncultured marrow mononuclear cells delivered within fibrin glue hydrogels to porous scaffolds enhance bone regeneration within critical-sized rat cranial defects. Tissue Eng Part A. 2010; 16:3555–68. [PubMed: 20715884]
7. Saiz E, Zimmermann EA, Lee JS, Wegst UG, Tomsia AP. Perspectives on the role of nanotechnology in bone tissue engineering. Dent Mater. 2013; 29:103–15. [PubMed: 22901861]
8. Rackwitz L, Eden L, Reppenhagen S, Reichert JC, Jakob F, Walles H, et al. Stem cell- and growth factor-based regenerative therapies for avascular necrosis of the femoral head. Stem Cell Res Ther. 2012; 3:7. [PubMed: 22356811]
9. Fong EL, Watson BM, Kasper FK, Mikos AG. Building bridges: leveraging interdisciplinary collaborations in the development of biomaterials to meet clinical needs. Adv Mater. 2012; 24:4995–5013. [PubMed: 22821772]
10. Ramalingam M, Young MF, Thomas V, Sun L, Chow LC, Tison CK, et al. Nanofiber scaffold gradients for interfacial tissue engineering. J Biomater Appl. 2013; 27:695–705. [PubMed: 22286209]
11. Thibault RA, Mikos AG, Kasper FK. Scaffold/extracellular matrix hybrid constructs for bone-tissue engineering. Adv Healthc Mater. 2013; 2:13–24. [PubMed: 23184883]
12. Klumpers DD, Zhao X, Mooney DJ, Smit TH. Cell mediated contraction in 3D cell-matrix constructs leads to spatially regulated osteogenic differentiation. Integr Biol (Camb). 2013; 5:1174. [PubMed: 23925497]
13. Lopez-Heredia MA, Pattipeilohy J, Hsu S, Grykien M, van der Weijden B, Leeuwenburgh SC, et al. Bulk physicochemical, interconnectivity, and mechanical properties of calcium phosphate

cements-fibrin glue composites for bone substitute applications. J Biomed Mater Res A. 2013; 101:478–90. [PubMed: 22927324]

14. Franco J, Hunger P, Launey ME, Tomsia AP, Saiz E. Direct write assembly of calcium phosphate scaffolds using a water-based hydrogel. Acta Biomater. 2010; 6:218–28. [PubMed: 19563923]
15. Bongio M, van den Beucken JJ, Nejadnik MR, Tahmasebi Birgani Z, Habibovic P, Kinard LA, et al. Subcutaneous tissue response and osteogenic performance of calcium phosphate nanoparticle-enriched hydrogels in the tibial medullary cavity of guinea pigs. Acta Biomater. 2013; 9:5464–74. [PubMed: 23107797]
16. Ambrosio L, Guarino V, Sanginario V, Torricelli P, Fini M, Ginebra MP, et al. Injectable calcium-phosphate-based composites for skeletal bone treatments. Biomed Mater. 2012; 7:024113. [PubMed: 22456083]
17. Habib M, Baroud G, Galea L, Bohner M. Evaluation of the ultrasonication process for injectability of hydraulic calcium phosphate pastes. Acta Biomater. 2012; 8:1164–8. [PubMed: 22075123]
18. Lopez-Heredia MA, Bongio M, Bohner M, Cuijpers V, Winnubst LA, van Dijk N, et al. Processing and in vivo evaluation of multiphasic calcium phosphate cements with dual tricalcium phosphate phases. Acta biomater. 2012; 8:3500–8. [PubMed: 22659172]
19. Perez RA, Kim TH, Kim M, Jang JH, Ginebra MP, Kim HW. Calcium phosphate cements loaded with basic fibroblast growth factor: delivery and in vitro cell response. J Biomed Mater Res A. 2013; 101:923–31. [PubMed: 22962037]
20. Grover LM, Wright AJ, Gbureck U, Bolarinwa A, Song J, Liu Y, et al. The effect of amorphous pyrophosphate on calcium phosphate cement resorption and bone generation. Biomaterials. 2013; 34:6631–7. [PubMed: 23747007]
21. Brown, WE.; Chow, LC. A new calcium phosphate water setting cement. In: Brown, PW., editor. Cements Research Progress. Westerville, OH: American Ceramics Society; 1986. p. 352-79.
22. Barralet JE, Gaunt T, Wright AJ, Gibson IR, Knowles JC. Effect of porosity reduction by compaction on compressive strength and microstructure of calcium phosphate cement. J Biomed Mater Res B. 2002; 63:1–9.
23. Ginebra MP, Driessens FC, Planell JA. Effect of the particle size on the micro and nanostructural features of a calcium phosphate cement: a kinetic analysis. Biomaterials. 2004; 25:3453–62. [PubMed: 15020119]
24. Bohner M, Baroud G. Injectability of calcium phosphate pastes. Biomaterials. 2005; 26:1553–63. [PubMed: 15522757]
25. Bodde EW, Habraken WJ, Mikos AG, Spauwen PH, Jansen JA. Effect of polymer molecular weight on the bone biological activity of biodegradable polymer/calcium phosphate cement composites. Tissue Eng Part A. 2009; 15:3183–91. [PubMed: 19364281]
26. Friedman CD, Costantino PD, Takagi S, Chow LC. BoneSource hydroxyapatite cement: a novel biomaterial for craniofacial skeletal tissue engineering and reconstruction. J Biomed Mater Res. 1998; 43:428–32. [PubMed: 9855201]
27. Xu HHK, Simon CG Jr. Fast setting calcium phosphate-chitosan scaffold: mechanical properties and biocompatibility. Biomaterials. 2005; 26:1337–1348. [PubMed: 15482821]
28. Ginebra MP, Traykova T, Planell JA. Calcium phosphate cements as bone drug delivery systems: a review. J Control Release. 2006; 113:102–10. [PubMed: 16740332]
29. Zhao L, Weir MD, Xu HHK. An injectable calcium phosphate-alginate hydrogel-umbilical cord mesenchymal stem cell paste for bone tissue engineering. Biomaterials. 2010; 31:6502–10. [PubMed: 20570346]
30. Chen W, Zhou H, Tang M, Weir MD, Bao C, Xu HHK. Gas-foaming calcium phosphate cement scaffold encapsulating human umbilical cord stem cells. Tissue Eng Part A. 2012; 18:816–27. [PubMed: 22011243]
31. Chen W, Zhou H, Weir MD, Tang M, Bao C, Xu HHK. Human embryonic stem cell-derived mesenchymal stem cell seeding on calcium phosphate cement-chitosan-RGD scaffold for bone repair. Tissue Eng Part A. 2013; 19:915–27. [PubMed: 23092172]
32. Levenberg S, Golub JS, Amit M, Itskovitz-Eldor J, Langer R. Endothelial cells derived from human embryonic stem cells. Proc Natl Acad Sci USA. 2002; 99:4391–6. [PubMed: 11917100]

33. Arpornmaeklong P, Brown SE, Wang Z, Krebsbach PH. Phenotypic characterization, osteoblastic differentiation, and bone regeneration capacity of human embryonic stem cell-derived mesenchymal stem cells. Stem Cells Dev. 2009; 18:955–68. [PubMed: 19327009]
34. de Peppo GM, Svensson S, Lenneras M, Synnergren J, Stenberg J, Strehl R, et al. Human embryonic mesodermal progenitors highly resemble human mesenchymal stem cells and display high potential for tissue engineering applications. Tissue Eng Part A. 2010; 16:2161–82. [PubMed: 20136402]
35. Lian Q, Lye E, Yeo S, Tan KW, Salto-Tellez M, Liu TM, et al. Derivation of clinically compliant MSCs from CD105+, CD24- differentiated human ESCs. Stem Cells. 2007; 25:425–36. [PubMed: 17053208]
36. Kuznetsov SA, Cherman N, Robey PG. In vivo bone formation by progeny of human embryonic stem cells. Stem Cells Dev. 2011; 20:269–87. [PubMed: 20590404]
37. Mateizel I, De Becker A, Van de Velde H, De Rycke M, Van Steirteghem A, Cornelissen R, et al. Efficient differentiation of human embryonic stem cells into a homogeneous population of osteoprogenitor-like cells. Reprod Biomed Online. 2008; 16:741–53. [PubMed: 18492382]
38. James D, Nam HS, Seandel M, Nolan D, Janovitz T, Tomishima M, et al. Expansion and maintenance of human embryonic stem cell-derived endothelial cells by TGFbeta inhibition is Id1 dependent. Nat Biotechnol. 2010; 28:161–6. [PubMed: 20081865]
39. Lee H, Shamy GA, Elkabetz Y, Schofield CM, Harrsion NL, Panagiotakos G, et al. Directed differentiation and transplantation of human embryonic stem cell-derived motoneurons. Stem Cells. 2007; 25:1931–9. [PubMed: 17478583]
40. Bielby RC, Boccaccini AR, Polak JM, Buttery LD. In vitro differentiation and in vivo mineralization of osteogenic cells derived from human embryonic stem cells. Tissue Eng. 2004; 10:1518–25. [PubMed: 15588411]
41. Hwang NS, Varghese S, Lee HJ, Zhang Z, Ye Z, Bae J, et al. In vivo commitment and functional tissue regeneration using human embryonic stem cell-derived mesenchymal cells. Proc Natl Acad Sci USA. 2008; 105:20641–6. [PubMed: 19095799]
42. Kim S, Kim SS, Lee SH, Eun Ahn S, Gwak SJ, Song JH, et al. In vivo bone formation from human embryonic stem cell-derived osteogenic cells in poly(d,l-lactic-co-glycolic acid)/hydroxyapatite composite scaffolds. Biomaterials. 2008; 29:1043–53. [PubMed: 18023477]
43. Jukes JM, Both SK, Leusink A, Sterk LM, van Blitterswijk CA, de Boer J. Endochondral bone tissue engineering using embryonic stem cells. Proc Natl Acad Sci USA. 2008; 105:6840–5. [PubMed: 18467492]
44. Smith LA, Liu X, Hu J, Ma PX. The enhancement of human embryonic stem cell osteogenic differentiation with nano-fibrous scaffolding. Biomaterials. 2010; 31:5526–35. [PubMed: 20430439]
45. Tang M, Chen W, Weir MD, Thein-Han W, Xu HHK. Human embryonic stem cell encapsulation in alginate microbeads in macroporous calcium phosphate cement for bone tissue engineering. Acta Biomater. 2012; 8:3436–45. [PubMed: 22633970]
46. Marx RE. Platelet-rich plasma: evidence to support its use. J Oral Maxillofac Surg. 2004; 62:489–96. [PubMed: 15085519]
47. Man Y, Wang P, Guo Y, Xiang L, Yang Y, Qu Y, et al. Angiogenic and osteogenic potential of platelet-rich plasma and adipose-derived stem cell laden alginate microspheres. Biomaterials. 2012; 33:8802–11. [PubMed: 22981779]
48. Hu Z, Peel SA, Ho SK, Sandor GK, Clokie CM. Platelet-rich plasma induces mRNA expression of VEGF and PDGF in rat bone marrow stromal cell differentiation. Oral Surg Oral Med Oral Pathol Oral Radiol Endod. 2009; 107:43–8. [PubMed: 18755609]
49. Langer HF, Stellos K, Steingen C, Froihofer A, Schönberger T, Krämer B, et al. Platelet derived bFGF mediates vascular integrative mechanisms of mesenchymal stem cells in vitro. J Molecular Cellular Cardio. 2009; 47:315–325.
50. Kasten P, Vogel J, Luginbuhl R, Niemeyer P, Weiss S, Schneider S, et al. Influence of platelet-rich plasma on osteogenic differentiation of mesenchymal stem cells and ectopic bone formation in calcium phosphate ceramics. Cells Tissues Organs. 2006; 183:68–79. [PubMed: 17053323]

51. Kasten P, Beverungen M, Lorenz H, Wieland J, Fehr M, Geiger F. Comparison of platelet-rich plasma and VEGF-transfected mesenchymal stem cells on vascularization and bone formation in a critical-size bone defect. Cells Tissues Organs. 2012; 196:523–33. [PubMed: 22796828]
52. Xu HHK, Quinn JB, Takagi S, Chow LC, Eichmiller FC. Strong and macroporous calcium phosphate cement: Effects of porosity and fiber reinforcement. J Biomed Mater Res. 2001; 57A: 457–466. [PubMed: 11523041]
53. Chen W, Liu J, Manuchehrabadi N, Weir MD, Zhu Z, Xu HHK. Umbilical cord and bone marrow mesenchymal stem cell seeding on macroporous calcium phosphate for bone regeneration in rat cranial defects. Biomaterials. 2013; 34:9917–25. [PubMed: 24054499]
54. Livak KJ, Schmittgen TD. Analysis of relative gene expression data using real-time quantitative PCR and the 2(-Delta Delta C(T)) Method. Methods. 2001; 25:402–8. [PubMed: 11846609]
55. Kim K, Dean D, Mikos AG, Fisher JP. Effect of initial cell seeding density on early osteogenic signal expression of rat bone marrow stromal cells cultured on cross-linked poly(propylene fumarate) disks. Biomacromolecules. 2009; 10:1810–1817. [PubMed: 19469498]
56. Verrier S, Meury TR, Kupcsik L, Heini P, Stoll T, Alini M. Platelet-released supernatant induces osteoblastic differentiation of human mesenchymal stem cells: potential role of BMP-2. Eur Cell Mater. 2010; 20:403–14. [PubMed: 21154246]
57. Yoshimi R, Yamada Y, Ito K, Nakamura S, Abe A, Nagasaka T, et al. Self-assembling peptide nanofiber scaffolds, platelet-rich plasma, and mesenchymal stem cells for injectable bone regeneration with tissue engineering. J Craniofac Surg. 2009; 20:1523–30. [PubMed: 19816290]
58. Nair MB, Varma HK, Menon KV, Shenoy SJ, John A. Reconstruction of goat femur segmental defects using triphasic ceramic-coated hydroxyapatite in combination with autologous cells and platelet-rich plasma. Acta Biomaterialia. 2009; 5:1742–55. [PubMed: 19297259]
59. Dong Z, Li B, Liu B, Bai S, Li G, Ding A, et al. Platelet-rich plasma promotes angiogenesis of prefabricated vascularized bone graft. J Oral Maxillofac Surg. 2012; 70:2191–7. [PubMed: 22365977]
60. Fennis JP, Stoelinga PJ, Jansen JA. Mandibular reconstruction: a histological and histomorphometric study on the use of autogenous scaffolds, particulate cortico-cancellous bone grafts and platelet rich plasma in goats. Int J Oral Maxillofac Surg. 2004; 33:48–55. [PubMed: 14690659]
61. Schlegel KA, Donath K, Rupprecht S, Falk S, Zimmermann R, Felszeghy E, et al. De novo bone formation using bovine collagen and platelet-rich plasma. Biomaterials. 2004; 25:5387–93. [PubMed: 15130723]
62. You TM, Choi BH, Li J, Jung JH, Lee HJ, Lee SH, et al. The effect of platelet-rich plasma on bone healing around implants placed in bone defects treated with Bio-Oss: a pilot study in the dog tibia. Oral Surg Oral Med Oral Pathol Oral Radiol Endod. 2007; 103:e8–12. [PubMed: 17275366]
63. Choi BH, Zhu SJ, Kim BY, Huh JY, Lee SH, Jung JH. Effect of platelet-rich plasma (PRP) concentration on the viability and proliferation of alveolar bone cells: an in vitro study. Int J Oral Maxillofac Surg. 2005; 34:420–4. [PubMed: 16053853]
64. Uggeri J, Belletti S, Guizzardi S, Poli T, Cantarelli S, Scandroglio R, et al. Dose-dependent effects of platelet gel releasate on activities of human osteoblasts. J Periodontol. 2007; 78:1985–91. [PubMed: 18062120]
65. Frechette JP, Martineau I, Gagnon G. Platelet-rich plasmas: growth factor content and roles in wound healing. J Dent Res. 2005; 84:434–9. [PubMed: 15840779]
66. Intini G. The use of platelet-rich plasma in bone reconstruction therapy. Biomaterials. 2009; 30:4956–4966. [PubMed: 19573909]
67. Gotz W, Reichert C, Canullo L, Jager A, Heinemann F. Coupling of osteogenesis and angiogenesis in bone substitute healing - a brief overview. Ann Anat. 2012; 194:171–3. [PubMed: 22055938]
68. Man Y, Wang P, Guo Y, Xiang L, Yang Y, Qu Y, et al. Angiogenic and osteogenic potential of platelet-rich plasma and adipose-derived stem cell laden alginate microspheres. Biomaterials. 2012; 33:8802–11. [PubMed: 22981779]
69. Perka C, Schultz O, Spitzer RS, Lindenhayn K, Burmester GR, Sittinger M. Segmental bone repair by tissue-engineered periosteal cell transplants with bioresorbable fleece and fibrin scaffolds in rabbits. Biomaterials. 2000; 21:1145–53. [PubMed: 10817267]

70. Shin H, Quinten Ruhe P, Mikos AG, Jansen JA. In vivo bone and soft tissue response to injectable, biodegradable oligo(poly(ethylene glycol) fumarate) hydrogels. Biomaterials. 2003; 24:3201–11. [PubMed: 12763447]

71. Leach JK, Kaigler D, Wang Z, Krebsbach PH, Mooney DJ. Coating of VEGF-releasing scaffolds with bioactive glass for angiogenesis and bone regeneration. Biomaterials. 2006; 27:3249–55. [PubMed: 16490250]

72. de Peppo GM, Svensson S, Lenneras M, Synnergren J, Stenberg J, Strehl R, et al. Human embryonic mesodermal progenitors highly resemble human mesenchymal stem cells and display high potential for tissue engineering applications. Tissue Eng Part A. 2010; 16:2161–82. [PubMed: 20136402]

73. Bilic J, Izpisua Belmonte JC. Concise review: Induced pluripotent stem cells versus embryonic stem cells: close enough or yet too far apart? Stem Cells. 2012; 30:33–41. [PubMed: 22213481]

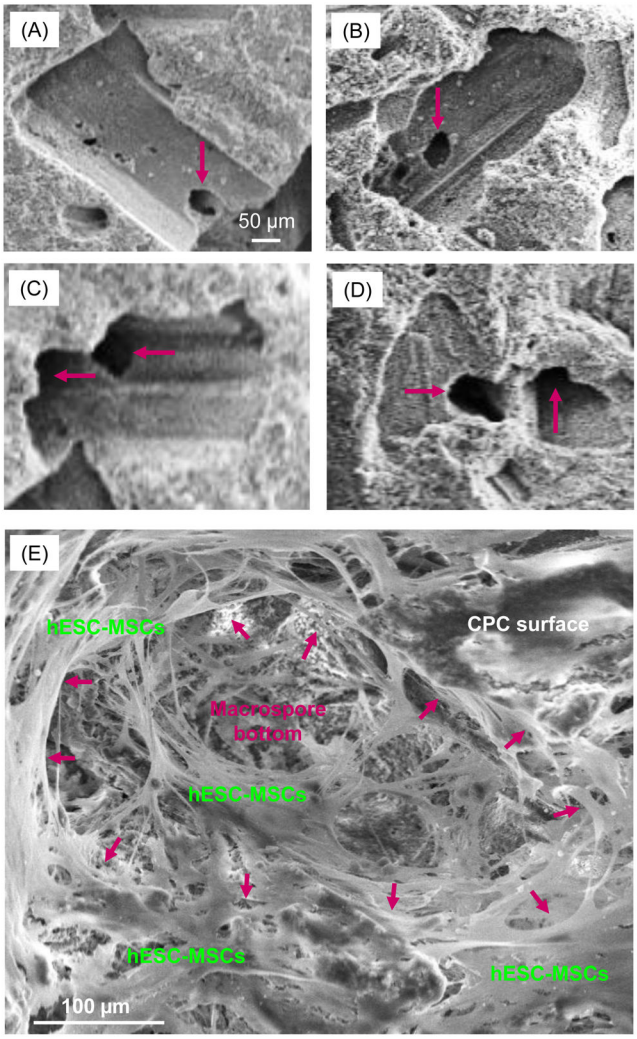

Figure 1.

Typical SEM images of CPC scaffolds: (A–D) before cell seeding, and (E) after hESC-MSC seeding and culturing for 7 d. Mannitol porogen dissolution in CPC created macropores in CPC. The pore volume fraction P of CPC was measured (mean ± sd; n = 5) to be (76 ± 3)%. Arrows in (A–D) indicate openings in the macropore walls and bottoms leading to the next macropores, indicating pore interconnection. The arrows in (E) indicate the approximate boundary of a macropore in CPC. Cells attached well to CPC and infiltrated into pores.

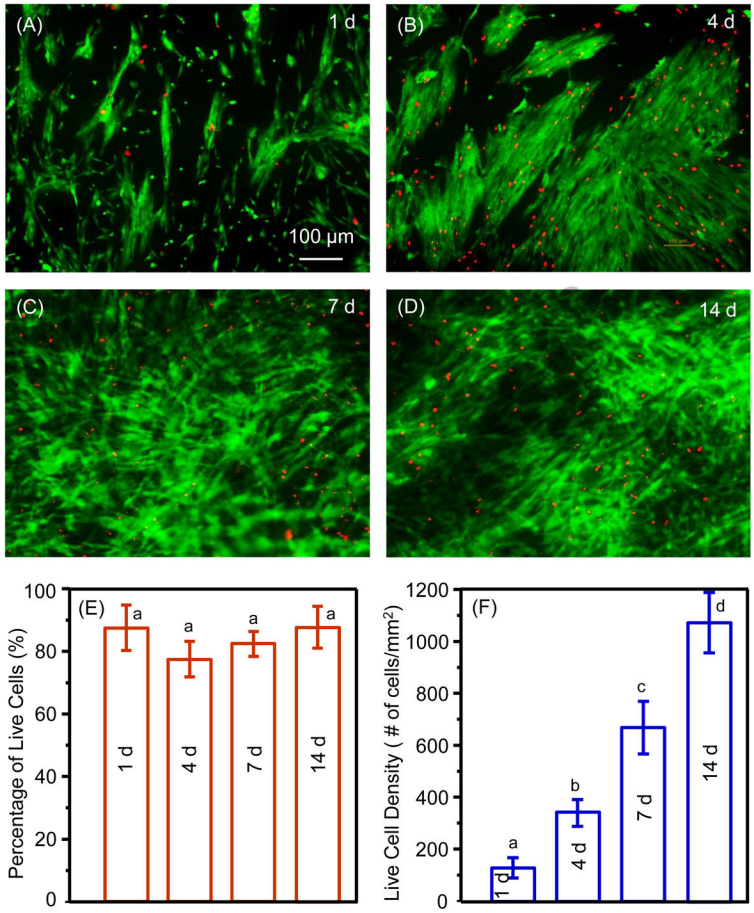

Figure 2.

Representative live/dead images of hESC-MSCs on CPC scaffolds cultured in osteogenic medium for (A) 1 d, (B) 4 d, (C) 7 d, and (d) 14 d. Live cells were stained green and dead cells were stained red. (E) Percentages of live cells (mean ± sd; n = 6), and (F) live cell density. In each plot, values with dissimilar letters are significantly different from each other ($p < 0.05$).

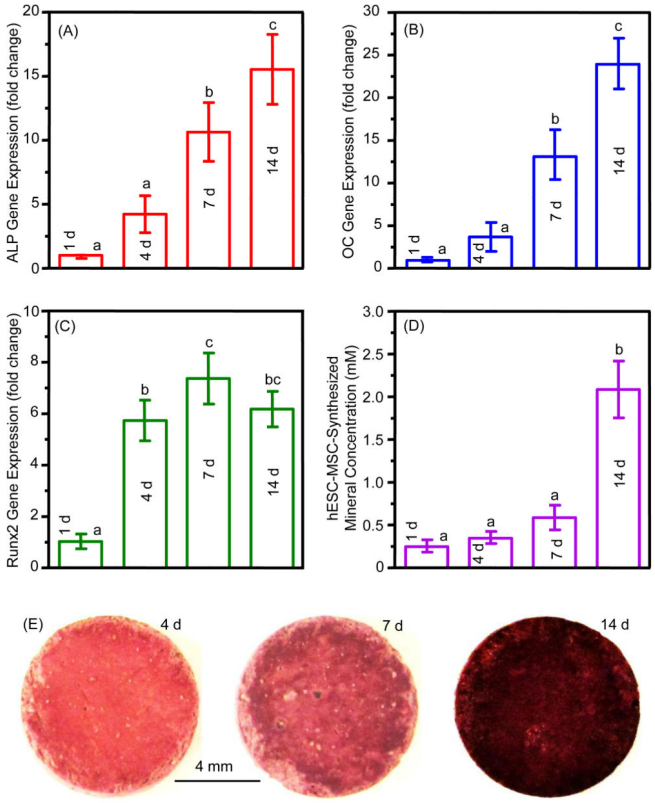

Figure 3.

Osteogenic differentiation of hESC-MSCs on CPC scaffolds (mean ± sd; n = 6). (A) Alkaline phosphatase (ALP) (F value = 34.145), (B) osteocalcin (OC) (F = 63.979), and (C) Runt-related transcription factor 2 (Runx2) gene expressions (F = 42.815). The C_t of hESC-MSCs cultured on CPC for 1 d served as the calibrator. (D) hESC-MSC-synthesized minerals (F = 58.727). (E) Representative photos of hESC-MSC-synthesized minerals stained red by ARS staining. Values with dissimilar letters are significantly different from each other ($p < 0.05$).

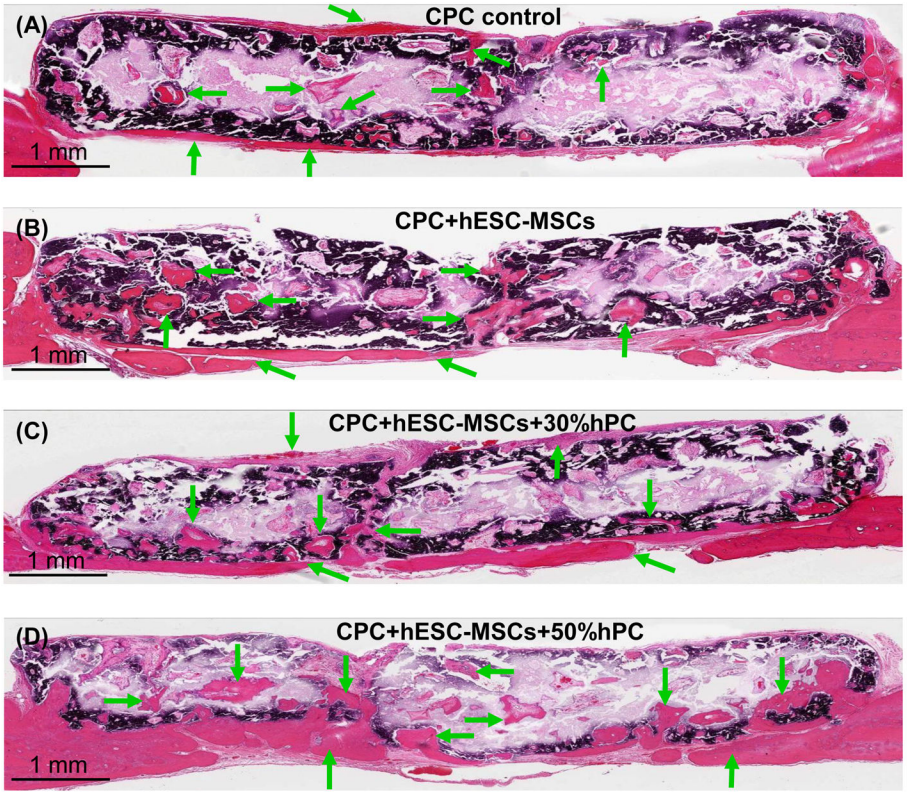

Figure 4.

Typical H&E images of the cross-sections of the critical-sized cranial defects in rats at 12 weeks. (A) CPC scaffold control without cells; (B) CPC seeded with hESC-MSCs (referred to as “CPC+hESC-MSC”; (C) CPC+hESC-MSC+30%hPC; and (D) CPC+hESC-MSC +50%hPC. Arrows indicate areas of new bone. There was more new bone in the groups with hESC-MSCs than CPC control without cells. There was more new bone when hPC was used, compared to that without hPC. The dark purple and white areas are residual CPC (the white areas were due to detachment of CPC during sample preparation). The dark purple staining of CPC was caused by incomplete decalcification in the CPC blocks during sample preparation.

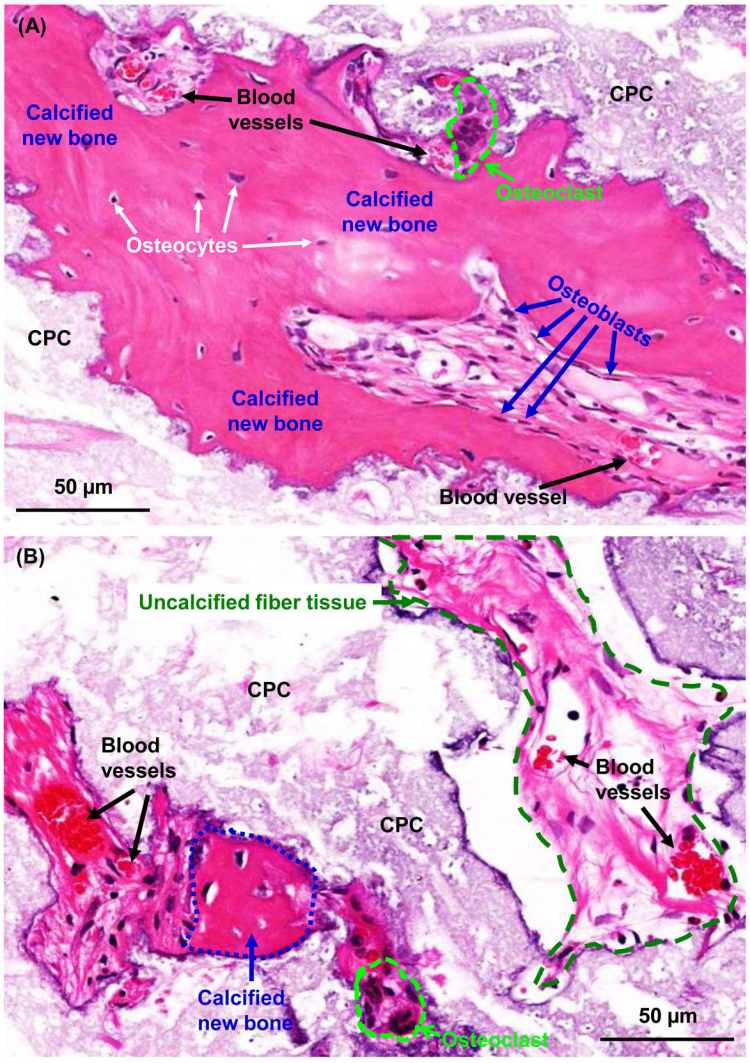

Figure 5.

High magnification H&E images. (A) New bone grew in the interior of CPC scaffold and was maturing as indicated by osteocytes and blood vessels. (B) Both calcified new bone and uncalcified new bone matrix were observed. Examples are shown for CPC+hESC-MSC +50%hPC; similar features were observed in other groups. The calcified new bone had a dark-red staining and a densely-organized matrix, with an example indicated by the blue line. The uncalcified tissue had a light-red staining with a loosely-structured matrix and was destined to be calcified over time in vivo, with an example indicated by the green line. Osteoclast-like multinuclear giant cells are encircled by light blue lines in both (A) and (B).

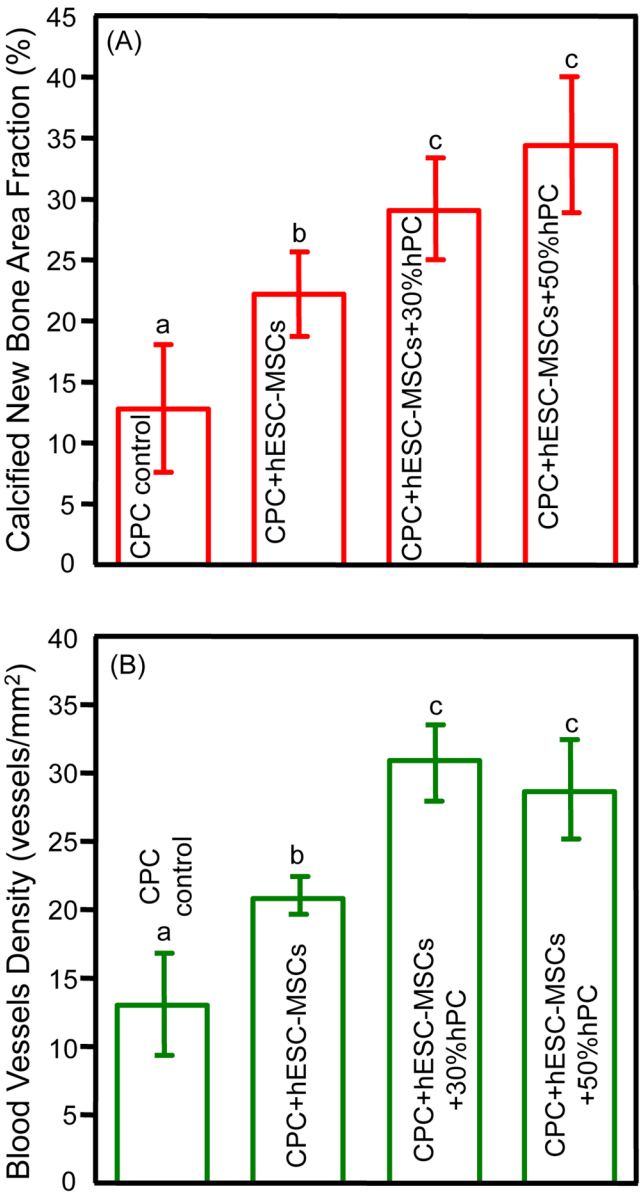

Figure 6.

Quantitative tissue regeneration results for critical-sized cranial defects in rats at 12 weeks (mean ± sd; n = 6): (A) Calcified new bone area fraction (F = 22.537), (B) new blood vessel density (F = 23.427). In each plot, values with dissimilar letters are significantly different from each other ($p < 0.05$). The groups seeded with hESC-MSCs and hPC had calcified new bone 3-fold, and blood vessel density 2-fold, those of CPC control.